Nonlocal effect of excited carriers on the bond strength of carbazole-based OLED host materials

Seunghyun Lee,[1,2] Noejung Park,[2] and Junhyeok Bang[1,3,*]

[1]*Spin Engineering Physics Team, Korea Basic Science Institute (KBSI), Daejeon 305-806, Republic of Korea*

[2]*Department of Physics, Ulsan National Institute of Science and Technology (UNIST), UNIST-gil 50, Ulsan 44919, Republic of Korea*

[3]*Department of Physics, Chungbuk National University, Cheongju 28644, Republic of Korea*

(Received 1 February 2020; accepted 23 March 2020; published 23 April 2020)

Despite the decades of development and successful implementations of organic light-emitting diodes (OLEDs) in various devices, the poor reliability mainly incurred by chemical degradations has remained a crucial issue. The overall mechanism of degradation has been outlined as an effect of excited carriers, and its microscopic details have yet to be understood. Here, using occupation-constrained density functional theory calculations, we investigate the role of excited carriers on the stability of OLED host materials. Unlike the electronic ground state, in which the chemical stability is mainly determined by the local atomic structure, the stability in the excited state is largely affected by the entire molecular structure, resulting in a nonlocal effect in the chemical degradation. Our results suggest the importance of this nonlocal effect in the excited state, represented by the excited carrier energy and potential energy landscape, to improve the reliability of the OLED device.

DOI: 10.1103/PhysRevMaterials.4.044603

Since the initial discovery of organic light-emitting diodes (OLEDs) in 1987 [1], remarkable technical development has been achieved, and recently, their successful applications reach wider range of commercial products, such as mobile displays and televisions [2–4]. Compared to other devices (e.g., liquid crystal display), OLEDs are characterized by several advantages, such as low power consumption, wide color gamut, compact structure, and light weight [5]. Moreover, the OLED fabrication cost has been positively forecasted as steadily reducing [6].

Despite its successful applications and advantages, the operational degradation (monotonic loss of luminance efficiency) and the poor device reliability remain challenging issues [7]. The degradation results from undesirable chemical reactions of organic molecules in the operating condition [8,9]. The reaction products can act as a charge trap or nonradiative recombination center, which significantly reduces device efficiency [10]. Furthermore, some products are highly reactive, which provokes additional chemical reactions with the surrounding molecules. Several experiments using mass spectrometry, liquid chromatography, and nuclear magnetic resonance have examined the pathways of the chemical reactions for several OLED host materials [7,11–14]. First-principles calculations have been applied to investigate the chemical stability of OLED molecules. The results indicated that the bond dissociation energies (BDEs), as a measure of the chemical stability, are low for C-S (∼2.9 eV), C-P (∼3.4 eV), and C-N bonds (∼3.5 eV); and within the assumption that the BDEs are determined by their local bonding structures, guidelines were suggested to minimize the number of such weak bonds when designing OLED molecules to improve the device reliability [6,14–19].

The chemical degradation occurs during the device operations, where the excited electron and hole carriers are injected from electrodes, and it is believed that the degradation is associated with the excited carrier [8,18–20]. However, most theoretical studies have considered BDEs within the Born-Oppenheimer surfaces of the electronic ground state. Recent works have considered the excitation effect, but they have simply compared the excitation energy of an initial structure with the BDE of the ground state and have considered the difference as a descriptor of the stability in the excited state [17,21,22]. To achieve more relevant descriptions of the chemical degradation process, a theoretical study directly accessing the effect of the excited carriers is highly necessary.

In this work, by using occupation-constrained density functional theory (DFT) calculations, we investigate the chemical degradation of OLED host materials (Fig. 1) in both electronic ground states and excited states. In the electronic ground state, BDE mainly depends on the local structure near the bond, and we observe that the BDEs of C-N and C-C bonds for the OLED host molecules are approximately 3.6 and 4.9 eV, respectively. In the electronic excited state, BDEs are significantly altered by the presence of excited carriers: (1) The BDEs are reduced by 2.1–3.2 eV from the values in the ground state. (2) In contrast to the ground state, the BDEs of C-N (0.75–1.38 eV) and C-C bonds (2.08–2.86 eV) show large variation among the molecules owing to the nonlocal effect of the excited carrier. (3) During the bond dissociation process, the energy surface exhibits a peak that is attributed to the crossing of excited state potential energy surfaces, whereas the total energy monotonically increases in the ground state. Our results indicate that, to improve the chemical stability, the whole molecular structure, beyond the local structure, should be considered for the optimal design of OLED molecules.

The optimized geometries and relevant energies of OLED host materials were obtained via spin-polarized DFT

*jbang@cbnu.ac.kr

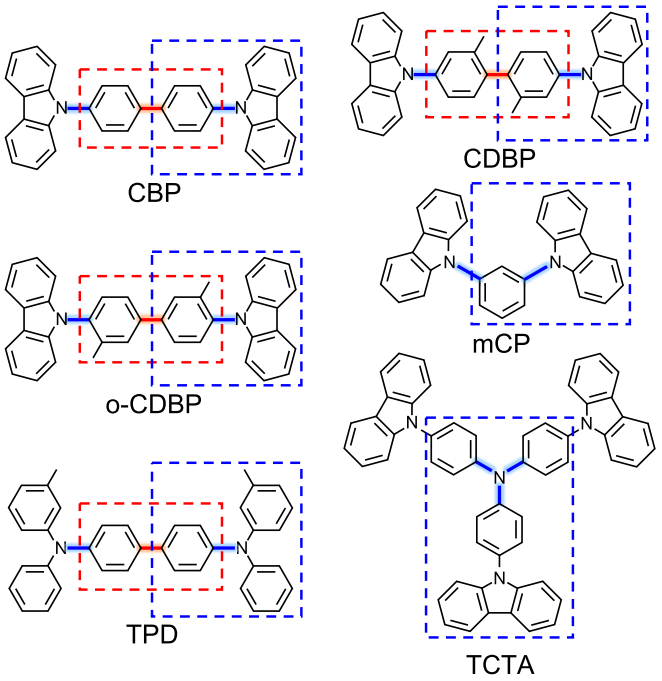

FIG. 1. Chemical structures of the OLED molecules. The dissociated C-N and C-C bonds are represented by blue and red lines, respectively, and their corresponding fragments are denoted by blue and red boxes, respectively.

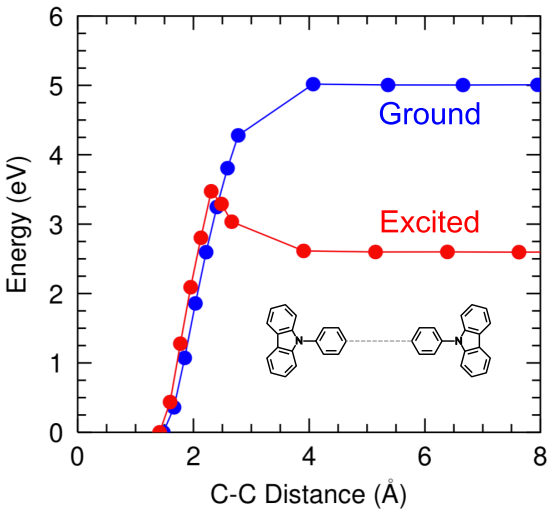

FIG. 2. Total energy variation in the C-C bond dissociation of the CBP molecule. Blue and red denote the electronic ground and excited state, respectively. The inset shows the atomic structure in the dissociation.

calculations within a generalized gradient approximation [23], as implemented in the Vienna *ab initio* simulation package [24]. Projector augmented wave potential [25] and a plane-wave basis set with an energy cutoff of 400 eV were employed. Most of the quantum chemistry calculations to date have employed atomic orbital basis sets, which are computationally less demanding than the plane-wave basis set. The reason that we used the plane-wave basis set is to remove the basis set superposition error [26], which is significant in the process of the chemical desorption. To prevent spurious interactions between neighboring cell images in the plane-wave calculations, we used a large supercell to ensure that the distances between the atoms in the neighboring cells exceeded 15 Å. As such, we removed the wave-function overlap between the neighboring cells, and our tests show that the total energy errors by the interactions between neighboring cells were below 0.01 eV. The ionic coordinates were fully relaxed until the residual forces were <0.02 eV/Å. We also performed vibrational frequency calculations for all relaxed structures, and we found no imaginary frequency. The bond stability was measured by BDE [6,14–19,21,22], obtained from the total energy difference between the original and dissociated structures. We also calculated the total energy variations with respect to the distance between the two fragments (Fig. 2). To identify the optimized pathway of the dissociation, we fix the distance between the two atoms participating in the bond, and the other atoms are fully relaxed.

To simulate the electronic excited state, we use occupation-constrained DFT calculations, in which we remove one electron from the highest occupied molecular orbital (HOMO) and place it at the lowest unoccupied molecular orbital (LUMO) [27,28]. When the excited carriers are injected from electrodes, they undergo ultrafast carrier-carrier or carrier-lattice scatterings within a picosecond, and the excited electron and hole are relaxed to the LUMO and HOMO, respectively [29]. Subsequently, the excited carriers remain at the LUMO or HOMO until they undergo recombination, for which the timescale is much slower (nano- or microsecond scale) than that of the scatterings. Thus, most of the injected carriers are in the LUMO and HOMO states, and the occupation-constrained DFT is a good approximation for describing the effect of the excited carriers in such a quasiequilibrium condition, where the chemical degradation occurs.

Figure 1 summarizes typical carbazole derivatives as representative OLED host materials that have widely been used as the emissive layer owing to their high triplet energies and hole mobility [10,30]. A 4,4′-bis(*N*-carbazolyl)-1,1′-biphenyl (CBP) is a typical hole-transporting host material [7,31–34], and its derivatives, such as 4.4′-bis(9-carbazolyl)-2,2′-dimethyl-biphenyl (CDBP), 4.4′-bis(9-carbazolyl)-3,3′-dimethyl-biphenyl (*o*-CDBP), and 1,3-bis(*N*-carbazolyl)benzene (mCP), have also been studied to improve their efficiencies and chemical stabilities [10,35,36]. In the present work, we additionally consider OLED hole-transporting materials such as *N*,*N*′-bis(3-methylphenyl)-*N*,*N*′-diphenylbenzidine (TPD) and tris(4-carbazoyl-9-ylphenyl)amine (TCTA).

Although reactions with chemicals from the surroundings, such as oxygen or water vapors, can in principle participate in the degradation process [8,21,37], in practice, the external sources can be circumvented by encapsulation. In these regards, we mainly focus on intrinsic dissociation processes. Among several possible bond dissociations, we ignore the dissociations of benzene and carbazole rings because the rings form stable aromatic π bonds, in addition to the σ bond [17,19]. Our main consideration is concentrated on the dissociations of the C-N and C-C bonds, which link the robust rings. The blue and red lines represent the C-N and C-C bonds,

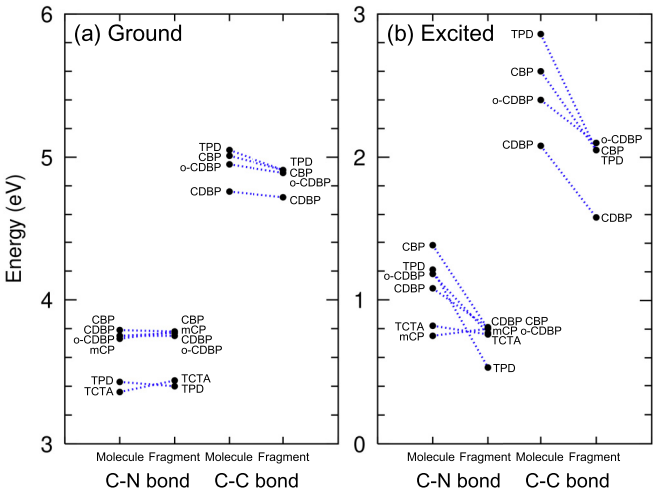

FIG. 3. C-N and C-C BDEs for molecules and fragments in (a) ground and (b) excited states. The variations of BDEs from molecules to fragments are represented by dotted blue lines.

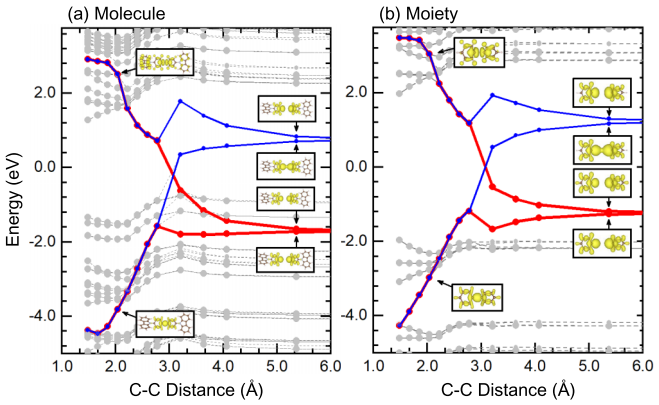

FIG. 4. Variations of energy level along with the C-C bond dissociation of (a) the CBP molecule and (b) the fragment. Red and blue indicate the majority and minority spin levels, respectively, of the C-C σ bonding and antibonding levels, and other background levels are represented in gray. The insets show the charge density of the corresponding level.

respectively, in Fig. 1. Note that the C-N and C-C linkages are relatively weak, and their BDEs are close to the energy of the singlet excited state [8,17–19,34]. The cleavage of these linkages has naturally been considered as the origin of the intrinsic chemical degradation [6,8,17,19].

We calculated the total energy profiles along the dissociation processes of the C-N and C-C linkages of the considered molecules. The cases of the C-C bond of CBP are presented in Fig. 2. In the electronic ground state, the total energies of all molecules monotonically increase with the bond elongation. As the only relevant parameter of the dissociation processes, we summarize the BDEs of the C-N and C-C bonds in Fig. 3 (see also Ref. [38]). The results, within 0.2 eV, are in good agreement with those of previous studies [38]. In the electronic ground state, the BDEs of the C-C bonds (averaged BDE = 4.94 eV) are higher than those of the C-N bonds (averaged BDE = 3.64 eV) by approximately 1.3 eV. The results are in good agreement with those of previous studies [6,14,16,18,19]. One important result is that, in the molecules, the standard deviations (σ) of C-N ($\sigma = 0.17$ eV) and C-C ($\sigma = 0.11$ eV) BDEs are very small. We note that, as shown in Fig. 3(a), only the C-N BDEs of TPD and TCTA are separated from those of the others (CBP, CDBP, *o*-CDBP, and mCP) by approximately 0.4 eV. This is also due to the different local structures around the N atom, i.e., biphenyl-diamine for TPD and phenylamine-carbazolyl for TCTA, but carbazole for the others (see Fig. 1). The small C-C BDE of CDBP relative to the others, as shown in Fig. 3(a), is also due to the local structure, i.e., the repulsive strain between nearby C and H atoms. These results clearly indicate that, *in the electronic ground state*, the chemical stability is mainly determined by the local structure around the bond.

The local effect of BDE is also clearly exhibited in fragments, which is the part of the molecule containing the dissociating bond, represented in Fig. 1. A dangling bond in the fragment is passivated using a hydrogen atom. As shown in Fig. 3(a) [38], the calculated C-N and C-C BDEs of the fragments are very similar to the corresponding values for the whole molecules. The differences are smaller than 0.08 eV for the C-N bond and 0.14 eV for the C-C bond, respectively. These results imply that the remote part of the molecules is insignificant in the BDEs. Previous studies have used this assumption, i.e., the local effect of BDE [6,16,21], to evaluate the stability of each bond based on calculations in a few representative fragments without considering various structures of whole molecules.

In the electronic excited state, both the C-N and C-C BDEs are significantly reduced, as shown in Fig. 3(b). This indicates that the chemical degradation can be activated in the device working condition. Compared to the electronic ground state, the variation of the C-N and C-C BDEs increases; BDEs lie in the range 0.75–1.38 eV for the C-N bond ($\sigma = 0.22$ eV) and 2.08–2.86 eV for the C-C bond ($\sigma = 0.29$ eV). The large variation in BDEs indicates that the effect of the excited carrier differs among the molecules. For the same C-N bonds, the BDE reduces by 2.98 eV in mCP and 2.22 eV in TPD, respectively. For the same C-C bonds, the BDE reduces by 2.68 eV for CDBP and 2.19 eV for TPD, respectively. Although the local structure near the bond (i.e., C-N or C-C) can lead to a large variation on the order of 1 eV in BDE (averaged C-N BDE = 1.07 eV and averaged C-C BDE = 2.49 eV), the nonlocal effect of the excited carrier can induce an energy variation on the order of 0.5 eV. For fine control of the OLED stability, such nonlocal effects should also be considered.

The nonlocal effect of the excited carrier is also clearly observed in the fragments. In contrast to the ground state, the BDE significantly changes from molecule to fragments in the excited state, as shown in Fig. 3(b). For example, the C-C BDEs of CBP are reduced from 2.60 eV (molecule) to 2.05 eV (fragment), whereas the corresponding change in the ground state is only 0.01 eV.

For a detailed analysis, we examined the variation of the energy level in the dissociation process: the case for the C-C bond of CBP is presented in Fig. 4. The results for other molecules are qualitatively the same and not shown. Among the molecular states below and above the Fermi level, the two

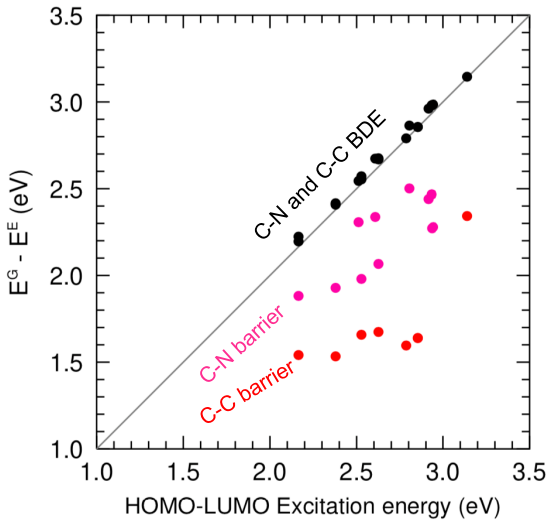

FIG. 5. Correlation between the HOMO-LUMO excitation energy and the reduction of BDEs (black), i.e., ${E_{BDE}}^G - {E_{BDE}}^E$, where ${E_{BDE}}^G$ and ${E_{BDE}}^E$ indicate the BDEs in the ground state and excited state, respectively. The corresponding correlations for the energy barriers, i.e., ${E_B}^G - {E_B}^E$, where ${E_B}^G$ and ${E_B}^E$ indicate the energy barrier in the ground state and excited state, respectively, are also presented in pink for the C-N bond and red for the C-C bond.

for majority spin and the two for minority spin, that exhibit a drastic variation on the bond elongation, are denoted by red and blue solid lines, respectively. The two occupied levels increase from −4.38 to −1.57 eV until 2.77 Å. Then, the two spin levels are split; the minority spin level increases further to 0.71 eV until 5.36 Å, and the majority spin level remains constant. In contrast, the evolution of the unoccupied molecular levels is the opposite; it decreases from 2.91 to 0.72 eV. Then, the majority spin level decreases further to −1.66 eV, and the minority spin level does not decrease further. Note that the large fluctuation at 3.2 Å is due to the change of the electron occupation. As shown in the insets in Fig. 4(a), these levels are the C-C σ bonding and antibonding states. Note that the variations of the other energy levels, denoted by gray dots and lines, are different, i.e., only increasing near 0.6 eV from 2 to 3 Å. This change is caused by the breaking of delocalized π bonds between the C atoms. The N π bonds in TPD and TCTA differ from those of the others (CBP, CDBP, *o*-CDBP, and mCP), as shown in Fig. 1. The different π local bond nature reduces the BDEs of TPD and TCTA by approximately 0.4 eV in the ground state.

Owing to ultrafast thermalization, as previously discussed, the excited electron and hole carriers are located at the HOMO and LUMO, respectively, which constitute the delocalized π bond. This delocalized nature of the excited carriers is the main cause of the nonlocal effect of BDE. The delocalized excited carrier is more confined in fragments than in molecules. Thus, the LUMO (HOMO) is pushed up (down) owing to the quantum confinement effect, as shown in Fig. 4(b), and consequently the excited carriers can reduce the BDE more in the fragments. Here, we show that the effect of the excited carriers can be quantified with the HOMO-LUMO excitation energy. The black points in Fig. 5 depict that the reduction of the BDE from the ground state to the excited state, ${E_{BDE}}^G - {E_{BDE}}^E$, where ${E_{BDE}}^G$ and ${E_{BDE}}^E$ are the BDEs in the ground and excited states, is well correlated to the HOMO-LUMO excitation energy.

As the C-C distance passes 2.3 Å, the C-C σ antibonding state drops below the LUMO, as shown in Fig. 4(a). In the excited state, the bond dissociation thus represents the electron transfer process from the LUMO to the C-C σ antibonding state, described by the Marcus-Hush theory [39,40]. This electron transfer induces the change of the potential energy surface, decreasing the system energy with the antibonding state after the crossing, which provides the underlying mechanism for the peak at 2.3 Å in the potential energy surface as shown in Fig. 2. We summarize the energy barrier in Table S1 in the Supplemental Material [38]. We also compare the HOMO-LUMO excitation energy with the reduction of the energy barrier from the ground state to the excited state, i.e., ${E_B}^G - {E_B}^E$, where ${E_B}^G$ and ${E_B}^E$ are the corresponding energy barriers in the ground and excited states, respectively. Here, the barrier for the ground state is the BDE, because there is no such peak in the ground-state potential energy surface. As shown in Fig. 5, the correlation of the energy barriers (pink for C-N bonds and red for C-C bonds) is relatively weaker than that of the BDE, because it involves a complicated electron transfer process. The C-C σ bond is stronger than the C-N σ bond, so the bonding (antibonding) level of the C-C bond is lower (higher) than that of the C-N bond. Therefore, the crossing of the energy levels occurs at a long C-C distance, and thus the reduction of the barrier of the C-C bond is smaller than that of the C-N bond. According to the Marcus-Hush theory [39,40], the nonadiabatic coupling at the crossing of energy surfaces is important for determining the charge transfer rate. Here, we consider the process only in the adiabatic limit. This is a good approximation in a timescale that is much slower than that of the carrier dynamics. Further studies are required to examine the nonadiabatic effect in the dissociation process.

In summary, by using the occupation-constrained DFT calculation, we investigated the chemical degradation of OLED molecules. In the device working condition, the excited carriers significantly weaken the C-N and C-C bonds, resulting in the chemical degradation. Interestingly, while the BDE is mostly determined by the bond itself (i.e., local effect), in the electronic ground state, the BDE in the electronic excited state is associated with the entire structure of the OLED molecules (i.e., nonlocal effect). The results suggest that the whole structure, not only the local atomic structure, should be considered to improve OLED device reliability.

This work was supported by Basic Science Research Program through the National Research Foundation of Korea (NRF) (NRF-2018R1D1A1B07044564), National Research Council of Science and Technology (Grant No. CAP-18-05-KAERI), and Korea Basic Science Institute (KBSI) Grant No. D39614. N.P. was supported by National Research Foundation of Korea (NRF-2017R1A4A1015323). We used the VESTA software to generate some of the figures [41].

[1] C. W. Tang and S. A. VanSlyke, Appl. Phys. Lett. **51**, 913 (1987).

[2] N. Chopra, J. Lee, Y. Zheng, S.-H. Eom, J. Xue, and F. So, Appl. Phys. Lett. **93**, 143307 (2008).

[3] M. E. Kondakova, T. D. Pawlik, R. H. Young, D. J. Giesen, D. Y. Kondakov, C. T. Brown, J. C. Deaton, J. R. Lenhard, and K. P. Klubek, J. Appl. Phys. **104**, 094501 (2008).

[4] S. H. Kim, J. Jang, K. S. Yook, and J. Y. Lee, Appl. Phys. Lett. **92**, 023513 (2008).

[5] L. Zhou, A. Wanga, S.-C. Wu, J. Sun, S. Park, and T. N. Jackson, Appl. Phys. Lett. **88**, 083502 (2006).

[6] W. Song and J. Y. Lee, Adv. Optical Mater. **5**, 1600901 (2017).

[7] D. Y. Kondakov, W. C. Lenhart, and W. F. Nichols, J. Appl. Phys. **101**, 024512 (2007).

[8] S. Scholz, D. Kondakov, B. Lussem, and K. Leo, Chem. Rev. **115**, 8449 (2015).

[9] R. Seifert, I. Rabelo de Moraes, S. Scholz, M. C. Gather, B. Lüssem, and K. Leo, Org. Electron. **14**, 115 (2013).

[10] Y. Tao, C. Yang, and J. Qin, Chem. Soc. Rev. **40**, 2943 (2011).

[11] S. Scholz, B. Lüssem, and K. Leo, Appl. Phys. Lett. **95**, 183309 (2009).

[12] S. Scholz, C. Corten, K. Walzer, D. Kuckling, and K. Leo, Org. Electron. **8**, 709 (2007).

[13] D. Y. Kondakov, J. Appl. Phys. **104**, 084520 (2008).

[14] S.-C. Dong, L. Xu, and C. W. Tang, Org. Electron. **42**, 379 (2017).

[15] N. Lin, J. Qiao, L. Duan, L. Wang, and Y. Qiu, J. Phys. Chem. C **118**, 7569 (2014).

[16] R. Wang, Y.-L. Wang, N. Lin, R. Zhang, L. Duan, and J. Qiao, Chem. Mater. **30**, 8771 (2018).

[17] A. Y. Freidzon, A. A. Safonov, A. A. Bagaturyants, D. N. Krasikov, B. V. Potapkin, A. A. Osipov, A. V. Yakubovich, and O. Kwon, J. Phys. Chem. C **121**, 22422 (2017).

[18] M. Hong, M. K. Ravva, P. Winget, and J.-L. Brédas, Chem. Mater. **28**, 5791 (2016).

[19] S. Schmidbauer, A. Hohenleutner, and B. Konig, Adv. Mater. **25**, 2114 (2013).

[20] F. So and D. Kondakov, Adv. Mater. **22**, 3762 (2010).

[21] J. Vijaya Sundar, V. Subramanian, and B. Rajakumar, Phys. Chem. Chem. Phys. **21**, 438 (2018).

[22] H. Li, M. Hong, A Scarpaci, X. He, C. Risko, J. S. Sears, S. Barlow, P. Winget, S. R. Marder, D. Kim, and J. L. Brédas, Chem. Mater. **31**, 1507 (2019).

[23] J. P. Perdew, K. Burke, and M. Ernzerhof, Phys. Rev. Lett. **77**, 3865 (1996).

[24] G. Kresse and J. Furthmüller, Comput. Mater. Sci. **6**, 15 (1996).

[25] P. E. Blochl, Phys. Rev. B **50**, 17953 (1994).

[26] K. Lee, J. Yu, and Y. Morikawa, Phys. Rev. B **75**, 045402 (2007).

[27] J. Bang, Z. Wang, F. Gao, S. Meng, and S. B. Zhang, Phys. Rev. B **87**, 205206 (2013).

[28] J. Bang, Y. Y. Sun, J. H. Song, and S. B. Zhang, Sci. Rep. **6**, 24404 (2016).

[29] S. K. Sundaram and E. Mazur, Nat. Mater. **1**, 217 (2002).

[30] K. S. Yook and J. Y. Lee, Adv. Mater. **24**, 3169 (2012).

[31] Y. H. Chen, C. C. Lin, M. J. Huang, K. Hung, Y. C. Wu, W. C. Lin, R. W. Chen-Cheng, H. W. Lin, and C. H. Cheng, Chem. Sci. **7**, 4044 (2016).

[32] X. Zhan, Z. Wu, Y. Lin, Y. Xie, Q. Peng, Q. Li, D. Ma, and Z. Li, Chem. Sci. **7**, 4355 (2016).

[33] R. Chavez III, M. Cai, B. Tlach, D. L. Wheeler, R. Kaudal, A. Tsyrenova, A. L. Tomlinson, R. Shinar, J. Shinar, and M. Jeffries-EL, J. Mater. Chem. C **4**, 3765 (2016).

[34] D. Kim, L. Zhu, and J.-L. Brédas, Chem. Mater. **24**, 2604 (2012).

[35] S. Tokito, T. Iijima, Y. Suzuri, H. Kita, T. Tsuzuki, and F. Sato, Appl. Phys. Lett. **83**, 569 (2003).

[36] J. He, H. Liu, Y. Dai, X. Ou, J. Wang, S. Tao, X. Zhang, P. Wang, and D. Ma, J. Phys. Chem. C **113**, 6761 (2009).

[37] A. P. Ghosh, L. J. Gerenser, C. M. Jarman, and J. E. Fornalik, Appl. Phys. Lett. **86**, 223503 (2005).

[38] See Supplemental Material at http://link.aps.org/supplemental/10.1103/PhysRevMaterials.4.044603 for the C-N and C-C bond dissociation energies of the molecules and corresponding fragments and comparison of BDEs between our calculations and previous works.

[39] R. A. Marcus, Rev. Mod. Phys. **65**, 599 (1993).

[40] R. A. Marcus, J. Chem. Phys. **24**, 966 (1956).

[41] K. Momma and F. Izumi, J. Appl. Crystallogr. **44**, 1272 (2011).